



CHORUS

This is the accepted manuscript made available via CHORUS. The article has been published as:

# Spin Splitting Unconstrained by Electron Pairing: The Spin-Vibronic States

Ungdon Ham and W. Ho

Phys. Rev. Lett. **108**, 106803 — Published 6 March 2012

DOI: [10.1103/PhysRevLett.108.106803](https://doi.org/10.1103/PhysRevLett.108.106803)

# Spin Splitting Unconstrained by Electron Pairing: The Spin-Vibronic States

Ungdon Ham and W. Ho \*

Department of Physics and Astronomy and Department of Chemistry  
University of California, Irvine, CA 92697-4575, USA

Spin-splitting of individual vibronic states was observed in a single molecule where all the electrons are paired, as well as a molecule with one extra electron injected. This observation was made possible by the use of a scanning tunneling microscope (STM) capable of reaching  $\sim 800$  mK in a magnetic field up to 9 Tesla and the sharpness of the vibronic states,  $\sim 1$  meV. These conditions also led to the resolution of spectral diffusion caused by minute fluctuations at the probing location of the molecule.

DOI:

PACS numbers: 68.37.Ef, 68.43.Pq, 73.40.Gk, 33.57.+c

\*To whom correspondence should be addressed. E-mail: [wilsonho@uci.edu](mailto:wilsonho@uci.edu)

The magnetic properties of atoms and molecules are determined by the occupation of electrons in the allowed energy states. The existence of a net spin associated with unpaired electrons is required for the widely used electron spin resonance (ESR) spectroscopy. In a magnetic field, the spin degeneracy is lifted and transitions between spin states occur by the emission and absorption of energy quanta. The sensitivity has even reached the level of single atoms and molecules with the detection of spin-flip excitation at  $\sim 1$  meV by inelastic electron tunneling spectroscopy (IETS) with the scanning tunneling microscope (STM) [1-3]. However, these measurements preclude a large number of molecules in which all the electrons are paired. Here we use the STM to obtain spin properties of single molecules without unpaired electrons by measuring the spin splitting of individual vibronic states. Our results demonstrate that magnetic properties can be obtained for all molecules irrespective of spin pairing. The experimental observation of spin-vibronic states points out a novel mechanism in spin dependent transport.

In STM-IETS, a step change in  $dI/dV$  is measured at the voltage corresponding to the threshold of an excitation [4]. Here, spin-splitting is observed for the different vibrational levels of the electronic states and thus represent qualitatively a different approach of probing the spin properties of single molecules [5]. Our experiment corresponds to resonant tunneling into spin-vibronic states and probes the coupling among electronic, vibrational, and spin properties of the molecule. In contrast to STM-IETS, peaks instead of steps are measured in  $dI/dV$  spectra. The observation is made possible by the sharpness of the vibronic states,  $\sim 1$  meV, obtained at  $\sim 800$  mK, and comparable spin splitting energy at 9 Tesla.

The experiment was carried out with a home-built ultrahigh vacuum STM (an adapted version of Reference 6) operated at 800 mK with magnetic field up to 9 Tesla applied perpendicular to the surface. Magnesium porphine (MgP) molecules were deposited by thermal

evaporation onto the partially oxidized NiAl(110) surface at  $\sim 20$  K (7,8). The effective temperature of 800 mK at the sample was obtained by fitting near-zero bias  $dI/dV$  spectra to the spin-flip IETS spectral function.

The MgP molecule exhibits reversible electron transfer that can be controlled with the bias voltage when it is adsorbed on the aluminum oxide surface [8]. In Fig. 1(a), as the bias is increased beyond  $\sim 0.5$  V, an electron is transferred from the tip into the lowest unoccupied molecular orbital (LUMO- $\alpha$ ) of the molecule. LUMO- $\alpha$  can accommodate two electrons. The added electron for the MgP<sup>-</sup> anion is in the singly occupied molecular orbital (SOMO), capable of accommodating only one electron, and is detected as the sample bias is decreased below  $\sim -0.3$  V. The threshold of the singly unoccupied molecular orbital (SUMO) is seen above the threshold for the LUMO- $\alpha$ . When the sample bias is decreased below the threshold for SOMO, the electron can be discharged from the MgP<sup>-</sup> back to the tip. The MgP<sup>-</sup> anion is stable on the oxide surface for  $\sim 1$  V between the charging and discharging, likely caused by local lattice distortions. The single unpaired electron in the MgP<sup>-</sup> anion is verified with the observation of spin-flip excitation by STM-IETS. In contrast, no such excitation is measured for the neutral MgP, indicating that all electrons are paired in the molecule.

The topographic STM image in Fig. 1(a) shows the spatial distribution of the SOMO of the MgP<sup>-</sup> anion for the associated molecular structure. The MgP molecule is sandwiched between the vacuum and the aluminum oxide in a double barrier tunnel junction connected to the metallic tip and NiAl(110) substrate (Fig. 1(a)). At the threshold of the SOMO and SUMO for the anionic MgP<sup>-</sup> and LUMO- $\alpha$  for the neutral MgP, series of sharp peaks in  $dI/dV$  are revealed (Fig. 1(b)-(d)) when the tunneling gap is decreased by setting it with lower magnitude of the bias voltage at 0.1 nA (1.375 V to  $-0.3$  V or 0.5 V) and a reduced rms bias modulation (15 mV to 1

mV) and step size (5 mV to 0.5 mV) compared to Fig. 1(a). Linear plots of the peak position in the  $dI/dV$  spectra versus the peak number are obtained (Fig. 1(e)-(g)) and the series are assigned to vibronic progressions [9]. The vibrational energies are obtained from the slopes of the linear plots. For the SOMO, the energies are 13 meV and 4 meV, with the latter being a progression on progression. The same 13 meV mode is resolved for the SUMO and LUMO- $\alpha$ . The 13 meV vibration is assigned to the out-of-plane, dome-type deformation of porphines when compared to the experimental value of  $108 \text{ cm}^{-1}$  (13.4 meV), which is in agreement with the calculated values of  $107 \text{ cm}^{-1}$  [10] and  $104 \text{ cm}^{-1}$  [11]. The 4 meV energy is compared to the calculated out-of-plane ruffle ( $39 \text{ cm}^{-1}$  or 4.7 meV) and saddle ( $37 \text{ cm}^{-1}$  or 4.6 meV) modes [11]. In the double barrier, the applied bias voltage is dropped across the vacuum and the oxide. The vibrational energies should be  $\sim 15\%$  less than the peak spacing obtained from the slopes in Fig. 1(e), (f), and (g) [9,12,13]. The corrected vibrational energies are 11 meV and 3.4 meV. The mode assignment remains valid since the differences are 1-2 meV from the measured or calculated values for isolated molecules and no other modes are close by in energy.

The vibronic peaks are resolved into doublets when the rms bias modulation is further decreased from 1 mV to 100  $\mu\text{V}$  and the scan step size is reduced from 0.5 mV to 50  $\mu\text{V}$  (Fig. 2). The doublet splitting is seen to depend linearly on the magnetic field for the third (Fig. 2(a)-(g)) and first (Fig. 2(h)-(n)) peaks in the vibronic spectrum of SOMO (corresponding to the first two vibronic states of the 13 meV progression.) The magnitude of the splitting  $\Delta_{\text{eff}}$  and its field dependence suggest the lifting of the electron spin degeneracy:  $\Delta_{\text{eff}} = g\mu_{\text{B}}B$ , where  $g$  is the  $g$ -factor,  $\mu_{\text{B}}$  is the Bohr magneton, and  $B$  is the applied magnetic field. From the slope of the plot of  $\Delta_{\text{eff}}$  versus  $B$ ,  $g = 2.13 \pm 0.26$  is obtained for the third vibronic peak of SOMO (Fig. 2(g)) and a

similar value of  $g = 2.22 \pm 0.11$  is measured for the first vibronic peak of SOMO (Fig. 2(n)). The voltage drops across the two tunneling barriers requires a decrease by  $\sim 15\%$  for  $\Delta_{\text{eff}}$  and hence  $g$ . Thus the  $g$ -factor is  $\sim 1.9$  because the bias voltage at the molecule is not precisely known.

The spin-vibronic splitting is also observed for the empty orbitals of SUMO for the anionic  $\text{MgP}^-$  (Fig. 3(a), (b)). In Fig. 3(a), spin-splitting of 1.3 meV is resolved for the first vibronic peak of SUMO at 9 T, but for the spectrum measured at 7 T (Fig. 3(b)), the doublet is not clear because of spectral diffusion that occurred during the average over multiple scans.

To study the nature of spectral diffusion further, we measured LUMO- $\alpha$  spectra on another MgP molecule (Fig. 3(c)-(h)). A composite of 72 single-scan  $dI/dV$  spectra reveals 5 groups (Fig. 3(c)), indicating the molecule is in different states separated in energy by  $\sim 0.5$  meV. These discrete spectral jumps are attributed to the phenomenon of spectral diffusion in single molecules caused by slight changes in the molecule and possibly in its environment [14]. It is possible to average multiple scans of  $dI/dV$  spectra without energy shifts because spectral diffusion is a random process (Fig. 3(c)), or selectively average those spectra that show the same energy position (Fig. 3(e)-(h)). The splitting for LUMO- $\alpha$ ,  $\Delta_{\text{eff}}$ , is shown to depend linearly on the magnetic field with  $g = 2.43 \pm 0.25$ , and with voltage division correction,  $g \sim 2.1$  (Fig. 3(h)). The observation of spin splitting for an unoccupied vibronic state of a neutral molecule without an unpaired electron demonstrates measurement of spin properties in molecules with zero electron spin magnetic moment.

While the energy splitting is given simply by  $\Delta_{\text{eff}} = g\mu_B B$ , the intensity of the spin-vibronic states depends on the spin-dependent tunneling dynamics. In the case of unoccupied orbitals, such as SUMO and LUMO- $\alpha$ , an electron with either spin orientation can tunnel through a spin-vibronic state:  $s_z = -1/2$  resonant tunnels into the lower energy vibronic state with

the spin magnetic moment aligned with the field, and  $s_z = +\frac{1}{2}$  into the higher state with moment opposite the field. Similar process occurs for molecular orbitals with paired electrons, such as fully occupied HOMO (not present here). There are two channels of tunneling involving  $s_z = \pm\frac{1}{2}$  for the electron from the substrate. The spin-dependent tunneling process occurs without changing the spin state of the molecule.

The case of spin splitting of SOMO proceeds with an additional inelastic tunneling channel because of the presence of an unpaired electron. For an electron tunneling from the substrate with  $s_z = -\frac{1}{2}$ , tunneling occurs without a change of state since the ground spin-vibronic state is singly occupied with an electron in the same spin orientation. When the substrate electron has  $s_z = +\frac{1}{2}$ , it has to have higher energy to access the empty spin-vibronic state. Because the SOMO can accommodate only one electron, the occupation of the higher spin-vibronic state forces the electron in the lower spin-vibronic state to leave. The net result of such a process leads to a final state that involves a spin-flip excitation in the molecule, corresponding to resonant inelastic electron tunneling spectroscopy.

High resolution tunneling spectroscopy has revealed the phenomenon of spectral diffusion and resolved spin splitting in single molecules without unpaired electrons. The magnitude of the splitting (including the g-factor) and the intensity of the peaks are expected to depend on the interaction of the spin-vibronic states with the magnetic field and the tunneling cross section. The spatial distributions of the spin, vibrational, and electronic states may further reveal the nature of the electron charge and spin and their couplings to the molecular vibrations. While spin-flip spectroscopy by STM-IETS probes single molecules with unpaired electrons, our results show that spin properties can be obtained for all molecules, including the larger fraction of molecules that do not have unpaired spins.

This work is supported by the National Science Foundation, under Grant No. DMR-0606520 and the NSF Instrumentation for Materials Research, under Grant No. DMR-0114246.

## References

- [1] A. J. Heinrich, J. A. Gupta, C. P. Lutz, and D. M. Eigler, *Science* **306**, 466 (2004).
- [2] X. Chen *et al.*, *Phys. Rev. Lett.* **101**, 197208 (2008).
- [3] N. Tsukahara *et al.*, *Phys. Rev. Lett.* **102**, 167203 (2009).
- [4] B. C. Stipe, M. A. Rezaei, and W. Ho, *Science* **280**, 1732 (1998).
- [5] Y.-S. Fu *et al.*, *Phys. Rev. Lett.* **103**, 257202 (2009). The possibility of Zeeman splitting of a vibronic state in a magnetic field was described and based on the splitting reported for one of several vibronic peaks of cobalt phthalocyanine multilayers self-assembled on Pb.
- [6] B. C. Stipe, M. A. Rezaei, and W. Ho, *Rev. Sci. Instrum.* **70**, 137 (1999).
- [7] A. Stierle *et al.*, *Science* **303**, 1652 (2004).
- [8] S. W. Wu, N. Ogawa, G. V. Nazin, and W. Ho, *J. Phys. Chem. C* **112**, 5241 (2008).
- [9] G. V. Nazin, S. W. Wu, and W. Ho, *Proc. Nat. Acad. Sci.* **102**, 8832 (2005).
- [10] P. M. Kozlowski *et al.*, *J. Phys. Chem. A* **103**, 1357 (1999).
- [11] H. H. Tsai and M. C. Simpson, *J. Phys. Chem. A* **107**, 526 (2003).
- [12] S. W. Wu, G. V. Nazin, X. Chen, X. H. Qiu, and W. Ho, *Phys. Rev. Lett.* **93**, 236802 (2004).
- [13] G. V. Nazin, X. H. Qiu, and W. Ho, *J. Chem. Phys. Comm.* **122**, 181105 (2005).
- [14] W. P. Ambrose and W. E. Moerner, *Nature* **349**, 225 (1991).

## Figure Captions

FIG. 1 (color online). STM topography and  $dI/dV$  spectroscopy measured at 9 T over a Mg porphine on  $\text{Al}_2\text{O}_3/\text{NiAl}(110)$ . (a) Single-scan  $dI/dV$  spectra. The thresholds for LUMO- $\alpha$ , SUMO, and SOMO, and single electron charging/discharging are indicated with arrows.

Tunneling gap: 1.375 V and 0.1 nA; rms bias modulation: 15 mV. Inset: topographic image (25 Å by 25 Å, -0.35 V and 0.1 nA) of  $\text{MgP}^-$ , molecular schematic ( $\times 2$  scale, same orientation as the image) and STM junction. Spectra in this paper used 311.11 Hz modulation frequency and were measured at the position indicated by the white circle in the image. (b) and (d) Averaged  $dI/dV$  spectra for the SOMO and the SUMO of  $\text{MgP}^-$ . Tunneling gap: -0.3 V and 0.1 nA; rms bias modulation: 1 mV. (c) Averaged  $dI/dV$  spectra for the LUMO- $\alpha$  of neutral MgP. Tunneling gap: 0.5 V and 0.1 nA; rms bias modulation: 1 mV. (e)-(g) Progressions of vibronic states in (b)-(d).

FIG. 2 (color online). Magnetic field dependence of (a)-(g) first and (h)-(n) third peaks of SOMO of  $\text{MgP}^-$ . Each  $dI/dV$  spectrum is average of 20 scans. Tunneling gap: -0.3 V and 0.1 nA; rms bias modulation: 100  $\mu\text{V}$ . The splitting  $\Delta_{\text{eff}}$  at each magnetic field was obtained by fitting the  $dI/dV$  spectrum with two Gaussian functions as shown in (a) and (h); the red curves represent the sum of the two Gaussian curves and fall on top of the data points.

FIG. 3 (color online).  $dI/dV$  spectra for the first peak of SUMO and LUMO- $\alpha$ . (a) and (b)  $dI/dV$  spectra averaged over 20 scans for the first peak of SUMO for  $\text{MgP}^-$  at 9 and 7 T, respectively.

Tunneling gap: -0.3 V and 0.1 nA; rms bias modulation: 100  $\mu\text{V}$ . In (b), splitting becomes unresolved because of spectral diffusion. (c) 72 single-scan  $dI/dV$  spectra for the first peak of LUMO- $\alpha$  of another neutral MgP at 7 T. Tunneling gap: -0.4 V and 0.1 nA; rms bias modulation: 100  $\mu\text{V}$ . The variations in the 72  $dI/dV$  spectra are caused by spectral diffusion and

classified into five groups: red, green, dark blue, light blue, and orange. The flat, featureless  $dI/dV$  spectra in black represent the molecule after a single electron charging during the measurement of these spectra. (d) Average of 72 spectra in (c). (e), (f) and (g)  $dI/dV$  spectra for the first peak of LUMO- $\alpha$  of neutral MgP at 9, 8, and 7 T by averaging 9  $dI/dV$  spectra from the group of dark blue color. Tunneling gap:  $-0.4$  V and  $0.1$  nA; rms bias modulation:  $100$   $\mu$ V. (h) Peak splitting  $\Delta_{\text{eff}}$ , obtained as in Fig. 2, vs. magnetic field for the first peak of LUMO- $\alpha$ .

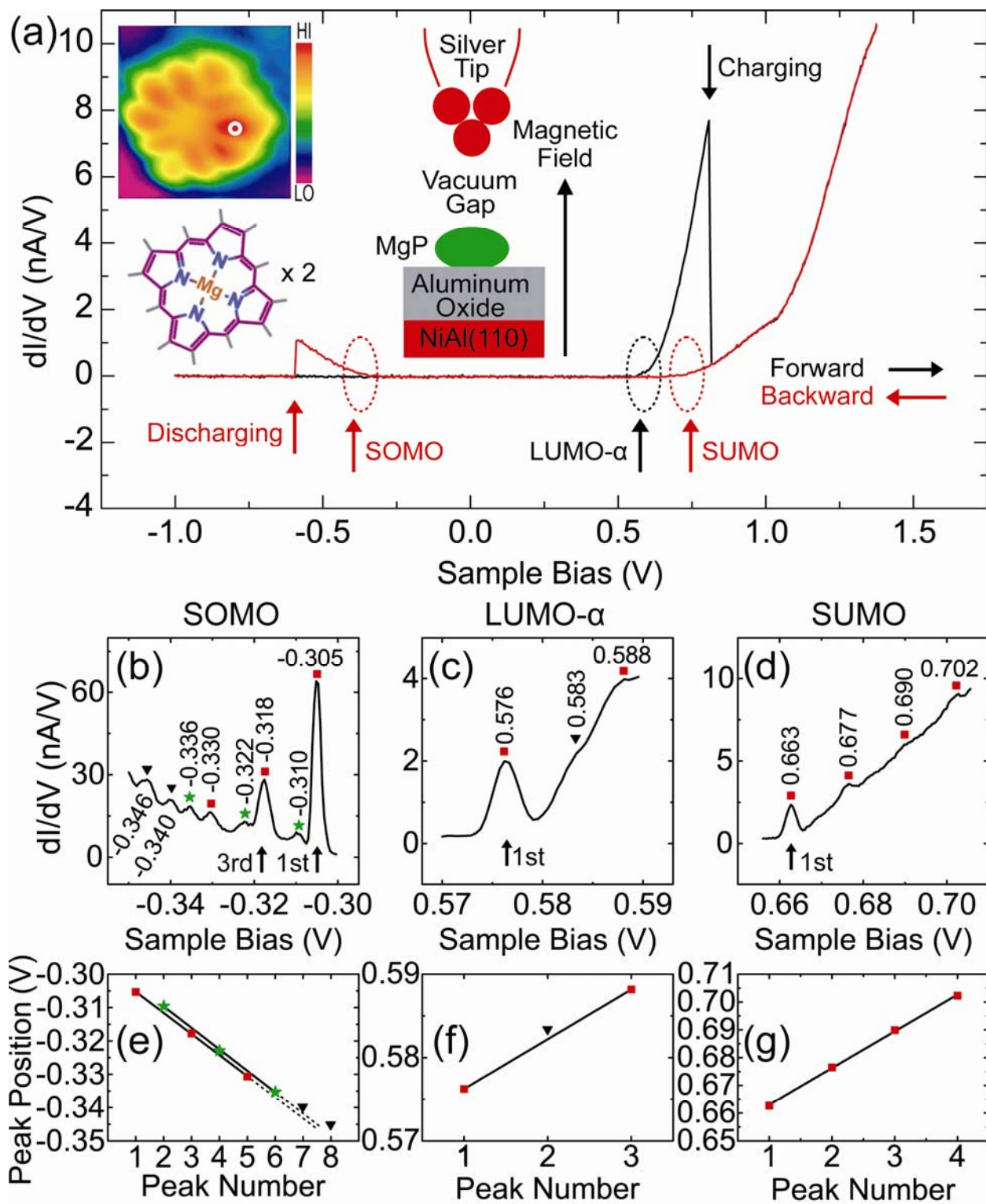


Figure 1

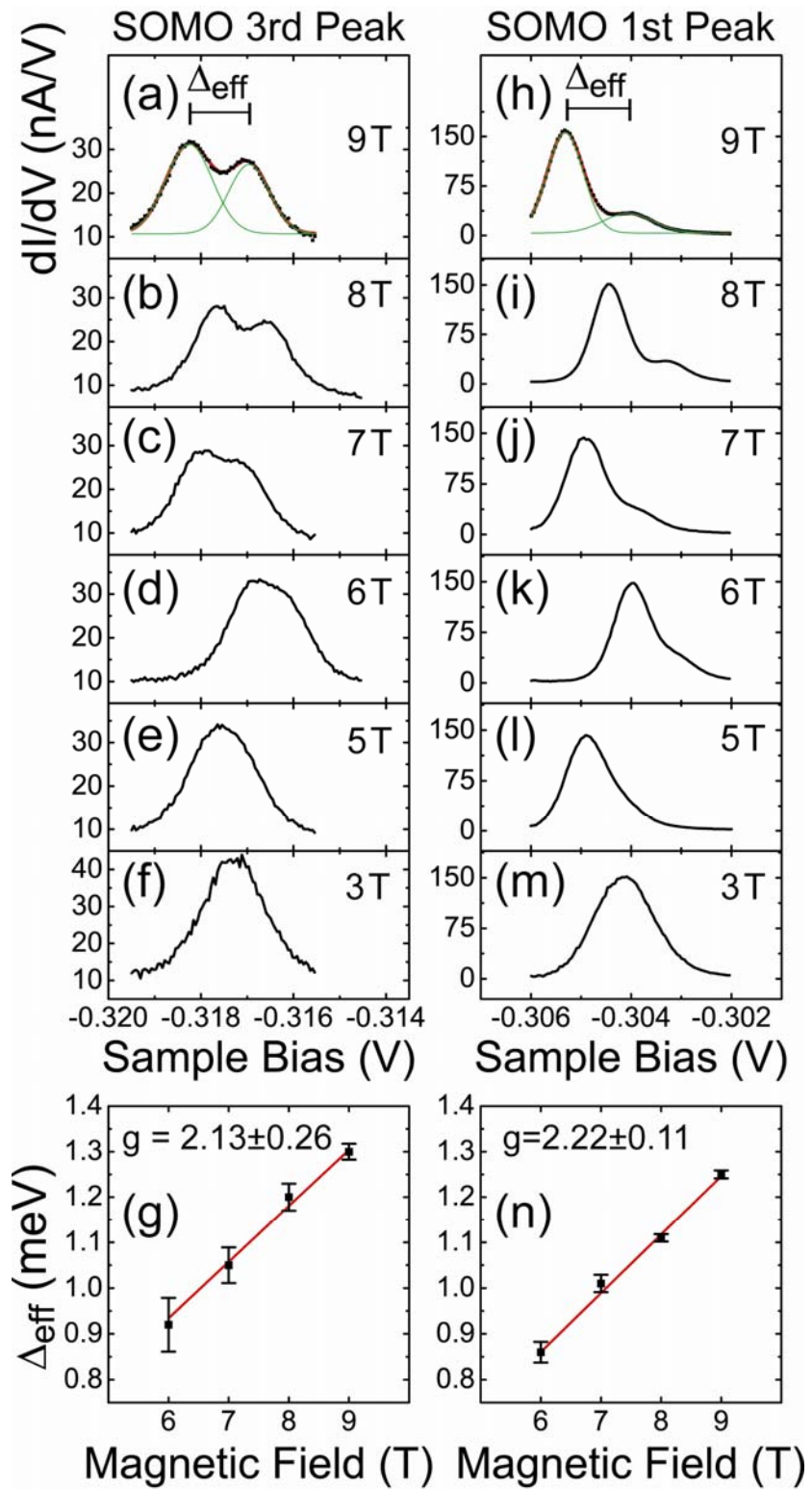


Figure 2

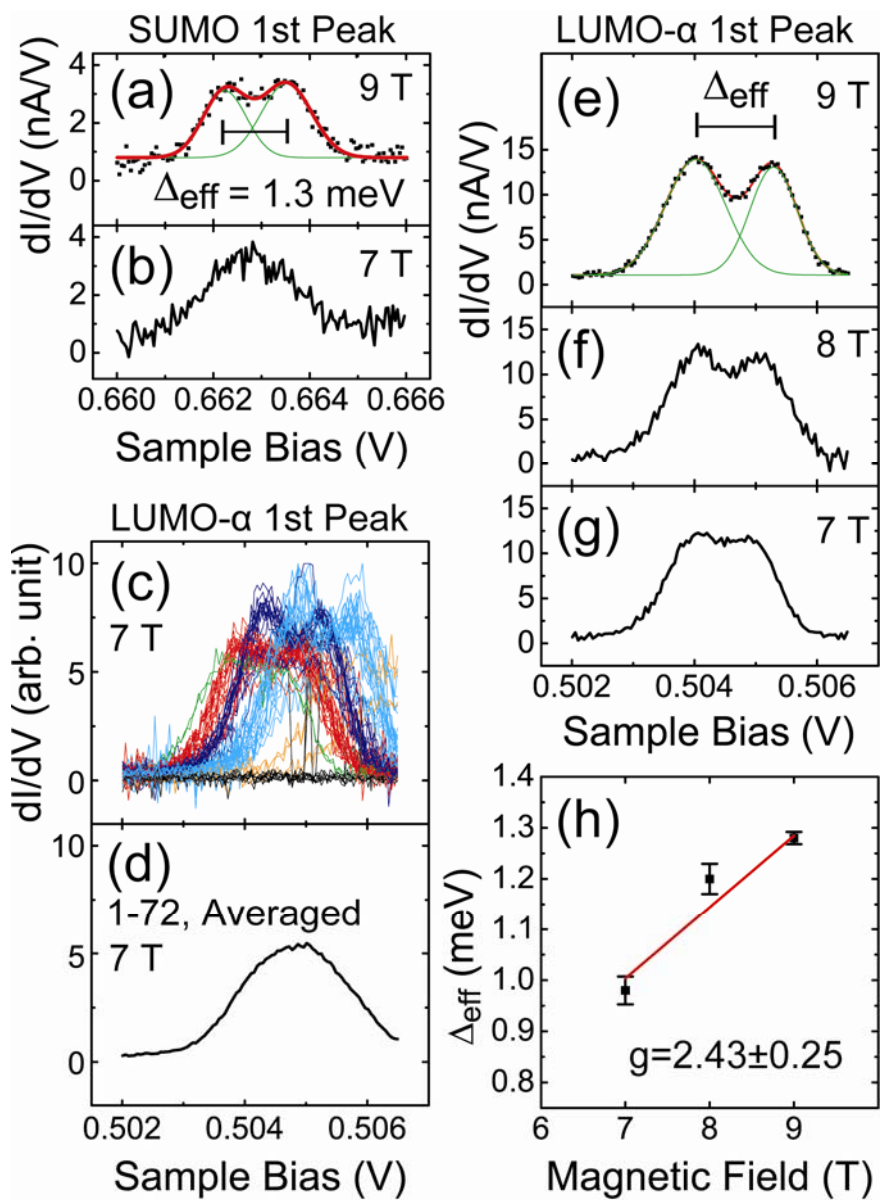


Figure 3